RSC Advances

ROYAL SOCIETY OF CHEMISTRY

www.rsc.org/advances

Journal Name

COMMUNICATION

Photocatalytic Hydrogen Evolution Based on Cu_2ZnSnS_4, $Cu_2ZnSnSe_4$, $Cu_2ZnSnSe_{4-x}S_x$ Nanofibers

Mehmet K. Gonce[a], Melike Dogru[b], Emre Aslan[b], Faruk Ozel[c], Imren Hatay Patir[b]*, Mahmut Kus[d], Mustafa Ersoz[b]

Received 00th January 20xx,

A new photocatalytic system for the hydrogen evolution from water has been reported by using a low cost and environment-friendly Cu_2ZnSnS_4, $Cu_2ZnSnSe_4$, $Cu_2ZnSnSe_{4-x}S_x$ nanofiber catalysts in the presence of eosin Y as a photosensitizer and a sacrificial reducing agent triethanolamine under visible light irradiation. The rate of hydrogen evolution with Cu_2ZnSnS_4 is greater than those with $Cu_2ZnSnSe_4$, $Cu_2ZnSnSe_{4-x}S_x$ by producing hydrogen 1428 $\mu molg^{-1}h^{-1}$, 833 $\mu molg^{-1}h^{-1}$ and 739 $\mu molg^{-1}h^{-1}$, respectively.

Photocatalytic production of hydrogen by water splitting is a promising strategy for converting solar energy into clean and carbon-free hydrogen fuel since it generates only water as a by-product during reaction with oxygen. A typical photocatalytic hydrogen evolution system consists of a sacrificial electron donor, a light-absorbing photosensitizer and proton reduction catalysts. So far, most of the photocatalytic systems employ noble metals as catalysts to achieve high photocatalytic activity [1-5]. For example, the systems comprising a xanthene dye Eosin Y (EY) sensitized with 1.0 wt% Pt-TiO_2, reported by Jin et.al, gave a hydrogen evolution rate of 12.7 $\mu molh^{-1}$(20 mg of catalyst)[6]. The considerable challenge is to develop robust catalysts composed of low-cost, earth-abundant elements that show activity comparable to that of the noble metals. Multicomponent chalcogenide semiconductors, namely Cu_2ZnSnS_4 (CZTS), $Cu_2ZnSnSe_4$ (CZTSe) and $Cu_2ZnSnSe_{4-x}S_x$(CZTSeS), have been found to be excellent candidate materials for application in photovoltaics [7,8] and thermoelectric [9] due to their advantages such as an optimum band gap (1.0–1.5 eV), high absorption coefficient, extremely low toxicity, and its components of only low-toxicity elements that are inexpensive and abundant in the Earth's crust. But apart from these applications, CZTS have also gained interest for the photocatalytic and electrocatalytic water splitting reactions. Recently, CZTS nanocrystals [10], CZTS nanosheets [11], CZTS-Pt and CZTS-Au heterostructured nanoparticles [12] have been investigated in the photocatalytic water splitting system. Kush et al. has been also reported that CZTS nanoparticles show high electrocatalytic activity for the hydrogen and oxygen evolution reaction [13]. In addition, we have shown that CZTS, Cu_2CoSnS_4 (CCTS) nanofibers exhibit highly comparable rates of catalysis to Pt particles for hydrogen evolution by using decamethylferrocene as an electron donor at water-DCE interfaces [14]. However, the catalytic behaviors of dye sensitized CZTS, CZTSe, CZTSeS nanofibers on the hydrogen evolution reaction activity are still not known and yet to be explored.

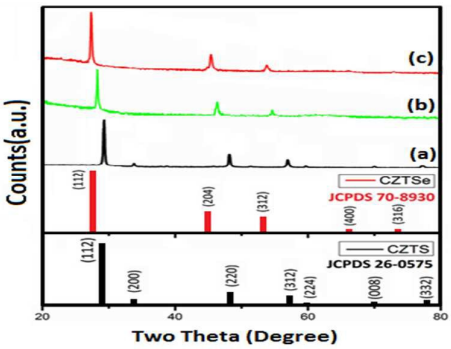

Figure 1. XRD patterns of as-fabricated CZTS (a, black line), CZTSe (c, red line), CZTSeS (b, green line) nanofibers. As references, the XRD patterns of CZTS (JCPDS 26-0575) and CZTSe (JCPDS 70-8930) from the standard ICCD are shown on the figure [15].

In this work, CZTS, CZTSe, CZTSeS nanofibers have been fabricated via a facile, two-step approach using a simple and inexpensive electrospinning technique as reported previously by our group [15]. An efficient photocatalytic system was constructed by using a noble metal-free CZTS, CZTSe, CZTSeS nanofibers as the catalyst with EY dye as the photosensitizer and triethanolamine (TEOA) as a sacrificial electron donor to give an efficient hydrogen evolution system under visible-light irradiation (λ > 420 nm). Herein, instead of noble metals, CZTS, CZTSe, CZTSeS nanofibers, for the first time, have been used as hydrogen evolution catalysts for the hydrogen generation from water in this photocatalytic system.

The synthesis of CZTS, CZTSe, CZTSeS nanofibers were carried out by electrospinning technique using polyacrilonitrile (PAN) as a templating polymer according to previously published procedure by our group [15] (see also SI section S-3 for the details). Figure 1 shows the XRD patterns of the fabricated CZTS, CZTSe and CZTSeS nanofibers.

[a] Selcuk University, Department of Nanotechnology and Advanced Materials, 42030, Konya, Turkey
[b] Selcuk University, Department of Chemistry, 42030, Konya, Turkey e-mail: imrenhatay@gmail.com Tel. +903322233898; Fax: +903322412499
[c] Karamanoglu Mehmetbey University, Department of Materials Science and Engineering, 70200, Karaman, Turkey
[d] Selcuk University, Department of Chemical Engineering, 42030, Konya, Turkey
† Supplementary Information (ESI) available: Experimental procedures, SEM images, Elemental mapping images, EDS spectrum, cyclic voltammograms, photocatalytic experiments See DOI: 10.1039/x0xx00000x

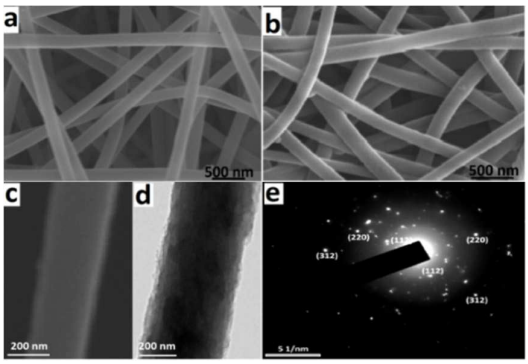

Figure 2. Scanning electron microscopy images of CuZnSn-PAN (CZT-PAN) nanofibers **(a)** and CZTS nanofibers **(b,c)**, Transmission electron microscopy images **(d)** and selected area diffraction pattern of CZTS nanofibers **(e)**.

The characteristic peaks of CZTS, CZTSe and CZTSeS are clearly observed on XRD patterns. All of the diffraction peaks of the crystallized nanofibers are both intense and neat, showing that the nanofibers have tetragonal structure with effective crystallization and lacking of impurity. The XRD peaks quietly shifted to higher angles as larger Se atoms are replaced by smaller S atoms. Since the coexistence of larger Se (1,98 Å) and smaller S (1,84 Å) atoms in sample, the diffraction values of ≈2° for CZTSeS nanofibers appear between CZTSe (JCPDS 70-8930) and CZTS (JCPDS 26-0575) values.

The scanning electron microscopy (SEM) images in Figure 2(a) shows that the CZT-PAN composite fibers were formed with good monodispersity and quite smooth structure, having an average diameter of 350 nm. CZT-PAN polymer-composite fibers were calcinated and chalcogenated to obtain CZTS, CZTSe and CZTSeS crystalline fibers (see SI Figure S-1 for the SEM images of CZTSe and CZTSeS). As the fibers were started to heat, all of the organic molecules in fiber structure began to decompose and left through evaporation as such forms of various gasses including carbon monoxide, carbon dioxide, hydrogen, nitrogen and others [15,16]. At the same time, crystallization was carried out and it was realized that fiber arrangement remained same while all of the fiber diameters decreased by approximately 100 nm (Figure 2 b-c). Figure 2(d) demonstrates a bright field transmission electron microscopy (TEM) image of as-fabricated CZTS fiber sample. Under TEM observation, the average diameter of fibers is observed to be around 250 nm, which is also confirmed by the SEM images. These results indicate that the form of fibers is not decomposed after chalcogenization and crystallization processes. The selected-area electron diffraction pattern (SAED) presented in Figure 2(e) matches with the structure of tetragonal CZTS and demonstrates that nanofibers have a single crystalline in nature (It is valid also for CZTSe and CZTSeS) [15,17].

Energy-dispersive X-ray spectroscopy (EDS) was performed to examine the overall homogeneity and composition of CuZnSnSeS as an example of the fabricated nanofibers. The EDS elemental mapping results also reveal that the individual elements (Cu, Zn, Sn, S and Se) of the fiber are homogeneously distributed throughout the fiber (See SI Figure S-2 and S-3). However, some dense regions which are, most probably, due to the aggregation of metal salts during electrospinning are also observed on the fiber surfaces. The average elemental composition ratio of Cu_2ZnSnS_4, $Cu_2ZnSnSe_4$ and $Cu_2ZnSn(SeS)_4$ nanofibers were found as $Cu_2Zn_1Sn_1S_4$, $Cu_2Zn_1Sn_1Se_4$ and$Cu_2Zn_1Sn_1(S_{0,66}Se_{0,34})_4$, respectively, which reveals that all samples are close to the ideal composition.

The optical properties of the nanofibers were monitored to determine the value of band gap structure**.** Absorption spectra of the nanofibers were recorded by dispersing the nanofibers in ethanol.

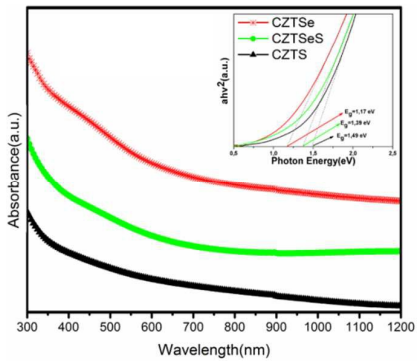

Figure 3. UV-Vis absorption spectrums, inset shows the calculated eV diagrams of CZTS, CZTSe and CZTSeS nanofibers.

As given in figure 3, the absorption spectra of CZTS, CZTSe and CZTSeS nanofibers exhibit a long tail covering a broad spectrum starting from the UV-visible region extending down to red region. For direct band gap compounds, the optical band gap can be calculated by plotting the product of photon energy and absorbance squared versus photon energy from the absorbance spectrum and finding the interrupt of the abscissa [18]. The optical band gaps of these CZTS, CZTSe and CZTSeS nanofibers were measured at around 1.49, 1.17 and 1,39eV, respectively.

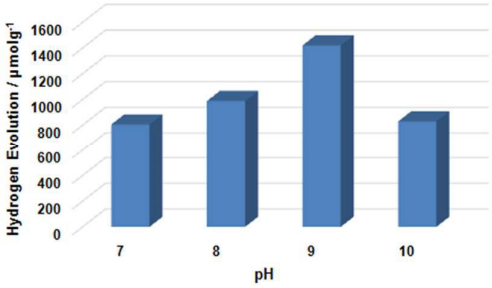

Figure 4. Influence of pH on the photocatalytic H_2evolution from the system comprising CZTS (10 mg), EY (3.25 10^{-4} M), and TEOA an electron donor (5%) in H_2O over 1 h irradiation.

Visible-light irradiation of the mixture of EY dye as a photosensitizer, sacrificial electron donor TEOA and CZTS, CZTSe or CZTSeS nanofibers as the catalyst resulted in a hydrogen evolution from water. The blank experiments indicated that all three components of the system (eosin Y, TEOA and nanofibers) are essential for H_2 production; no H_2 produced in the absence of anyone of them. First, the influence of the solution pH on the H_2 evolution reaction was explored with the system of TEOA (5%, v/v), EY (3.25 10^{-4} M) and CZTS nanofiber (10 mg) in water for 1 h irradiation of visible light. As can be seen from figure 4, the pH value of the medium considerably affects the photoinduced H_2 evolution. The amount of H_2 generation reaches to the maximum of

1428 μmolg^{-1}h^{-1} at pH 9 and decreases at both more acidic and more basic pH values. The decrease of H_2 production at acidic pH results from the protonation of TEOA which would lead to diminished efficiency of TEOA as a sacrificial electron donor. In the case of more basic pH values, the protonation of the CZTS nanofibers would be unfavorable which are consistent with those previous works [19,20].

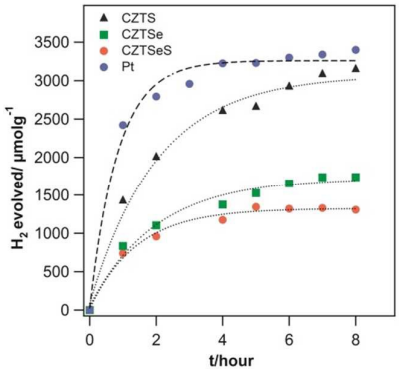

Figure 5. Time courses of the photocatalytic hydrogen production of CZTS, CZTSe and CZTSeS nanofibers (the amount of nanofibers is 10 mg, EY (3.25 10^{-4} M) and TEOA (5%) in 20 ml H_2O at pH=9). The hydrogen evolution activity of nanofibers has been also compered to that of Pt under the same conditions with 1.2 wt % Pt).

Figure 5 shows reaction time courses of hydrogen evolution by using TEOA (5%, v/v), EY (5%, v/v) and CZTS, CZTSe or CZTSeS nanofibers (10mg) at pH 9 in water under irradiation of visible light. It has been shown that CZTS nanofibers exhibit enhanced catalytic activity in comparison with the CZTSe and CZTSeS nanofibers, giving 1428 μmolg^{-1}h^{-1}, 833 μmolg^{-1}h^{-1} and 739 μmolg^{-1}h^{-1}, respectively. When a sample of CZTS, CZTSe or CZTSeS nanofibers is irradiated in water solution in the presence of TEOA, EY solution at pH 9 for 24 h, they produce a total of 3 mmolg^{-1}, 1.7 mmolg^{-1} and 1.3 mmolg^{-1} of H_2, respectively. Moreover, the catalytic hydrogen evolution activity by CZTS nanofibers shows comparable rates of catalysis to Pt particles. From the figure 5, it can be seen that the hydrogen evolution ceases after about 8 h. To understand the reason of deactivation, the change of absorption spectra of EY was investigated before and after visible light irradiation. As shown in figure S-4 (see SI), the strong characteristic absorption peak at 520 nm for EY before irradiation shifts to about 490 nm and it is very weak after irradiated by visible light for 8 h, which indicates that the sensitizer EY may be almost completely degraded during the reaction [13,21]. Another reason for the deactivation of the catalytic activity may be also due to the probable photocorrosion of this p-type semiconductors and Cu (I) is metastable phase in aqueous solution [10].

The difference between hydrogen evolutions rates of CZTS, CZTSe or CZTSeS nanofibers could be attributed to the conduction band (CB) levels. The mechanism of hydrogen generation and CB levels of nanofibers is illustrated in figure 6. EY (E_{ox}=0.89 V vs. normal hydrogen electrode (NHE) [22]) molecules absorb light to form the excited state of *EY (-1.1 V [23]). Electrons released from *EY are transferred to the CB of CZTS, CZTSe and CZTSeS nanofibers, -0.67 V, -0.81 V,-0.83 V for the hydrogen evolution reaction (nanofibers play role as an electron acceptor) (see SI figure S-5 for the cyclic voltammetry measurements). This reaction occur easily due to the CB levels of the nanofibers which are more negative than the reduction potential of H^+/H_2 (-0.41 vs NHE) [24]. The difference in redox potential between proton and nanofibers decrease in the order of CZTS, CZTSe and CZTSeS, respectively. Hydrogen evolution activity also increases in an expected order. Moreover, the excited state electron injection from eosin Y to semiconductors is the fastest step [25]. In the hydrogen evolution reaction, the most important step is the transfer of electrons between the semiconductors and H_2O. As pointed out by Morrison [26], electrons can only be transferred between those energetic states in the semiconductor and the electrolyte that are at approximately the same energy level [27]. Among CZTS, CZTSe and CZTSeS nanofibers, the nearest band level to H_2O/H_2 reduction potential is CZTS nanofibers. The CB levels of the CZTSe and CZTSeS are close to each other and so follow similar trend for the hydrogen evolution as shown in figure 5. It has been stated above that CZTS nanofibers do not show any photocatalytic hydrogen evolution activity in the absence of eosin dye. Therefore, CZTS nanofibers act as the only catalyst instead of photocatalyst in our reaction system.

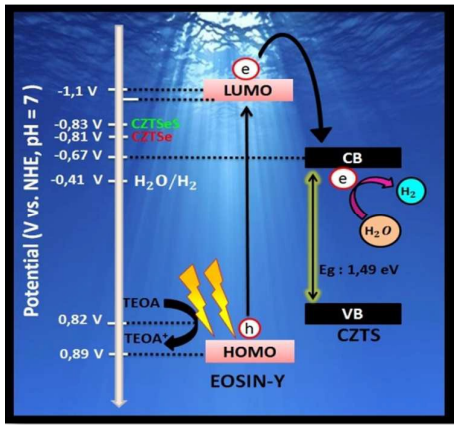

Figure 6. Proposed mechanism for photocatalytic hydrogen evolution over EY sensitized CZTS nanofibers.

Conclusions

In this work, the photocatalytic hydrogen evolution activity based on dye sensitized CZTS, CZTSe, CZTSeS nanofibers have been firstly reported. The fabricated nanofibers by electrospinning process are well-ordered and have uniform diameter of 250 nm. Moreover, CZTS, CZTSe, CZTSeS nanofibers have good crystallinity and homogeneous atomic dispersivity. CZTS, CZTSe and CZTSeS nanofibers serve as good catalysts as an alternative to noble metals for EY-sensitized hydrogen production from water under visible light. The hydrogen evolution rate of CZTS nanofibers is higher than that of CZTSe, CZTSeS nanofibers, which could be attributed to the conduction band levels of the nanofibers. Thus we may suggest that such highly efficient, inexpensive and abundant catalyst offer new opportunities for a variety of applications in the fields of energy conversion systems instead of noble metals.

Acknowledgements

The authors would like to thank TUBITAK (The Scientific and Technological Research Council of Turkey) (211T185 and 214M366), the COST Action (MP1106), TUBA (Turkish Academy of Sciences) and Karamanoglu Mehmetbey Universty**,** Scientific Research Council for supporting this work. This paper is the part of MSc thesis prepared by Mehmet Kerem Gonce and Melike Dogru which also supported by Selcuk University**,** Scientific Research Projects (BAP).

Notes and references

1 P. Lei, M. Hedlund, R. Lomoth, H. Rensmo, O. Johansson and L. Hammarstrom, *J. Am. Chem. Soc.*, 2008, **130**, 26–27.
2 L. L. Tinker, N. D. McDaniel, P. N. Curtin, C. K. Smith, M. J. Ireland and S. Bernhard, *Chem.–Eur. J.*, 2007, **13**, 8726–8732.
3 S. M. Arachchige, J. R. Brown, E. Chang, A. Jain, D. F. Zigler, K. Rangan and K. J. Brewer, *Inorg. Chem.*, 2009, **48**, 1989–2000.
4 S. Tschierlei, M. Karnahl, M. Presselt, B. Dietzek, J. Guthmuller, L. Gonzalez, M. Schmitt, S. Rau and J. Popp, *Angew. Chem. Int. Ed.*, 2010, **49**, 3981–3984.
5 H. Ozawa, Y. Yokoyama, M. Haga and K. Sakai, *Dalton Trans*., 2007, **12**, 1197–1206.
6 Z. Jin, X. Zhang, Y. Li, S. Li and G. Lu, *Catal. Commun.*, 2007, **8**, 1267–1273.
7 H. Zhou, W. C. Hsu, H. S. Duan, B. Bob, W. Yang, T. B. Song, C. J. Hsu and Y. Yang, *Energy Environ. Sci.*, 2013, **6**, 2822-2838.
8 F. Fan, L. Wu and S. Yu, *Energy Environ. Sci.*, 2014, **7**, 190-208.
9 S. Ji, T. Shi, X. Qiu, J. Zhang, G. Xu, C. Chen, Z. Jiang and C. Ye, *Scientific Reports,* 2013, **3**, 2733.
10 J. Wang, P. Zhang, X. Song and L. Gao, *RSC Adv.*, 2014, **4**, 27805-27810.
11 L. Wang, W. Wang and S. Sun, *J. Mater. Chem*, 2012, **22**, 6553–6555.
12 X. Yu, A. Shavel, X. An, Z. Luo, M. Ibanez and A. Cabot, *J. Am. Chem. Soc.*, 2014, **136**, 9236–9239.
13 P. Kush, K. Deori, A. Kumar and S. Deka, *J. Mater. Chem. A*, 2015, **3**, 8098-8106.
14 F. Ozel, A. Yar, E. Aslan, E. Arkan, A. Aljabour, M. Can, I. H. Patir, M. Kus and M. Ersoz, *ChemNanoMat*, Manuscript Number:cnma.201500113, under review
15 F. Ozel, M. Kus, A. Yar, E. Arkan, M. Z. Yigit, A. Aljabour, S. Büyükcelebi, C. Tozlu and M. Ersoz, *Materials Letters*, 2015, **140**, 23-26.
16 F. Ozel, M. Kus, A. Yar, E. Arkan, M. Can, A. Aljabour, N. M. Varal, M. Ersoz, *J Mater Sci.,* 2015, **50**, 777-783.
17 S. S. Mali, P. S. Patil and C. K. Hong, *ACS Appl. Mater. Interfaces*, 2014, **6**, 1688.
18 L. Chen and Y. Chuang, *Journal of Power Sources*, 2013, **241**, 259.
19 B. Flynn, W. Wang, C. Chang and G. S. Herman, *Phys. Status Solidi A*, 2012, **209**, 2186–2194.
20 X. Zhang, Z. Jin, Y. Li, S. Li and G. Lu, *Journal of Power Sources*, 2007, **166**, 74-79.
21 X. Zhang, Z. Jin, Y. Li, S. Li and G. Lu, *J. Colloid and Interface Science*, 2009, **333**, 285-293.
22 M. Yin, S. Ma, C. Wu and Y. Fan, *RSC Adv*., 2015, **5**, 1852-1858.
23 X. Chen, S. Shen, L. Guo, and S. S. Mao, *Chem. Rev.*, 2010, **110**, 6503-6570.
24 S. K. Choi, S. Kim, J. Ryu, S. K. Lim and H. Park, *Photochem. Photobiol. Sci*., 2012, **11**, 1437.
25 S. Ardo, G. J. Meyer, *Chem. Soc. Rev.*, 2009, **38**, 115–164.
26 S.R. Morrison, *The Chemical physics of surfaces*, Springer Science+Business Media, Second Edition, 1990, 438.
27 Y. Xu, M.A.A. Schoonen , *American Mineralogist* 2000, **85**, 3-4, 543–556.

